Limit Analysis of Shells with Part-Through Thickness Defects

A.G. Miller

Berkeley Nuclear Laboratories, Central Electricity Generating Board, Berkeley, Gloucestershire GL13 9PB, U.K.

SUMMARY

The integrity of structures containing defects may be obtained from interpolation between a linear elastic fracture mechanics analysis for brittle failure and limit analysis for ductile failure. In order to make this assessment there is a need for limit analysis of structures with defects. In the case of the primary pressure containment of reactors, these structures will be some form of shells. As exact limit solutions are rare, use is usually made of the bounding theorems of limit analysis, which depend on either satisfying equilibrium and yield, or compatibility and the flow rule. Shell theory implies approximations to all these aspects. Moreover, the yield function and associated flow rule are often further simplified to make the problem tractable. Mathematically the problem is one of programming, for which algorithms exist, though the efficiency of these when applied to limit analysis varies greatly.

The unusual feature considered here is the behaviour of the defect. Conventional shell theory ignoring shear strain in the through thickness direction is inadequate to describe the behaviour at the defect. This is similar to LEFM calculations, where it is found that conventional eighth order Kirchhoff elastic shell theory gives stress intensity factor predictions that are significantly in error when compared to the results from tenth order Reissner elastic shell theory, where the shear strain is not neglected. However, the method adopted here is to retain the conventional Kirchhoff theory, except at the defect itself, where a more detailed treatment is used. The results may be illustrated by the limit pressure of axisymmetric geometries. The solution methods may be ad hoc for a particular problem, or general, and both types were used. Two general purpose programs were written, using the two bounding theorems. These used finite differences to approximate the equilibrium and compatibility equations, and a linearised version of the yield surface and flow rule. The limit pressure was then determined using linear programming. Ad hoc methods were also used, where the global stress and velocity fields were constructed in terms of a small number of parameters, which were determined by non-linear optimization, with the pressure being the function to be optimized. The limit pressure was also determined experimentally. For small test pieces made from mild steel, the fracture of the ligament at the defect is governed by plastic collapse.

1. INTRODUCTION

The ductile failure of pressure vessels containing defects is considered here. This is a process governed by plastic instability, and may be represented approximately by limit analysis. For thick walled water reactors, the failure is dominated by LEFM. However, in the thinner-walled gas-cooled reactors, ductile failure becomes significant, and the two different mechanisms may be combined in a two-criteria structural integrity assessment. (Dowling and Townley [9]). This approach has been developed by the CEGB as the "R6" method (Harrison, Loosemore, Milne and Dowling [10]).

A compendium of limit solutions for cracked structures has been drawn up, covering the following geometries (Miller [8]).

1) plates under tension and bending and various defect geometries.
2) cylinders with internal pressure and various defect geometries.
3) spheres with internal pressure and various defect geometries.
4) sphere-cylinder intersections with internal pressure and defect round intersection.
5) pipe bends under in-plane bending with various defect geometries.

As an illustration of the method, two axisymmetric shell geometries are considered here. The first is a sphere with a fully circumferential part-through defect on a small circle. The second is a sphere with a protruding radial cylindrical nozzle, with an external defect in the sphere at the intersection. The limit pressure for each geometry has been calculated by three different theoretical methods. The theoretical results for the spheres are compared with experimental results.

2. NOMENCLATURE

n component in direction of normal to shell.

p ratio of limit pressure to membrane limit pressure for plain shell.

r_o small circle radius.

r_1 meridional radius of curvature.

t thickness

t_N nozzle thickness

v velocity

L defect radius, nozzle radius L_N nozzle length

M bending moment stress resultant

M_o $\frac{1}{4}\sigma_y t^2$

N tensile force stress resultant

N_o $\sigma_y t$

P pressure

Q shear force stress resultant

$\dot{W}_e$ external work rate

β rotation of normal

γ shear strain

ε tensile strain

ζ -1/+1 for external/internal defects

η fractional ligament thickness

θ longitude

κ change in curvature

ρ $L/\sqrt{r_1 t}$

σ_y yield stress

ϕ co-latitude

3. SHELL BEHAVIOUR

The limit analysis of axisymmetric shells has been described by Hodge [1]. The equilibrium relationships are:

$$\frac{1}{r_o r_1}\frac{d(r_o N_\phi)}{d\phi} - \frac{N_\theta \cos\phi}{r_o} - \frac{Q_\phi}{r_1} = 0 \tag{1}$$

$$\frac{1}{r_o r_1}\frac{d(r_o Q_\phi)}{d\phi} + \frac{N_\theta \sin\phi}{r_o} + \frac{N_\phi}{r_1} = P \tag{2}$$

$$\frac{1}{r_o r_1}\frac{d(r_o M_\phi)}{d\phi} - \frac{M_\theta \cos\phi}{r_o} - Q_\phi = 0 \tag{3}$$

The strain displacement relationships are:

$$\dot{\varepsilon}_\theta = \frac{v_\phi \cos\phi}{r_o} + \frac{v_n \sin\phi}{r_o} \tag{4}$$

$$\dot{\varepsilon}_\phi = \frac{1}{r_1}\frac{dv_\phi}{d\phi} + \frac{v_n}{r_1} \tag{5}$$

$$\dot{\gamma}_\phi = -\frac{v_\phi}{r_1} + \frac{1}{r_1}\frac{dv_n}{d\phi} + \dot{\beta}_\phi \tag{6}$$

$$\dot{\kappa}_\theta = \frac{\dot{\beta}_\phi \cos\phi}{r_o} \tag{7}$$

$$\dot{\kappa}_\phi = \frac{1}{r_1}\frac{d\dot{\beta}_\phi}{d\phi} \tag{8}$$

Sign conventions are arbitrary, provided these relationships satisfy the virtual work equation. In shell theory it is conventionally assumed that the shear strain rate $\dot{\gamma}_\phi$ is zero, and the associated shear stress resultant Q_ϕ becomes a passive reaction.

The external work done by the pressure is

$$\dot{W}_e = \int P 2\pi r_o \, v_n \, r_1 \, d\phi \tag{9}$$

In the axisymmetric case, the above relations are well-defined within the assumptions of shell theory. The only common modification is to ignore Q_ϕ in the first equilibrium equation. However the yield criterion is not so well-defined. There is no exact analytic representation of the shell equivalents of the Tresca and Mises continuum yield criteria. The two most common approximate yield criteria for axisymmetric shells (where the principal directions are known a priori) are the two-moment limited interaction yield surface,

$$\left|\frac{N_\theta}{N_o}\right| \leq 1 \qquad \left|\frac{N_\phi}{N_o}\right| \leq 1 \qquad \left|\frac{N_\theta - N_\phi}{N_o}\right| \leq 1 \tag{10}$$

$$\left|\frac{M_\theta}{M_o}\right| \leq 1 \qquad \left|\frac{M_\phi}{M_o}\right| \leq 1 \qquad \left|\frac{M_\theta - M_\phi}{M_o}\right| \leq 1 \tag{11}$$

and the sandwich yield surface:

$$\left|\frac{N_\theta}{N_o} \pm \frac{M_\theta}{M_o}\right| \leq 1 \qquad \left|\frac{N_\phi}{N_o} \pm \frac{M_\phi}{M_o}\right| \leq 1 \qquad \left|\frac{N_\theta - N_\phi}{N_o} \pm \frac{M_\theta - M_\phi}{M_o}\right| \leq 1 \tag{12}$$

Associated with each of these yield surfaces is the corresponding flow rule, and the corresponding internal work rate may be calculated. These respectively circumscribe and inscribe the Tresca yield surface, and so produce bounds to the Tresca limit pressure. Alternatively the limited interaction surface gives a good approximation so long as bending and stretching are not simultaneously important, and the sandwich yield surface applies to a shell of sandwich construction.

4. DEFECT BEHAVIOUR

Only surface defects are considered here, although the method may be adapted easily to include buried defects. The defect is simply taken to be a position where the shell thickness is locally thinner, and the ligament is eccentric with respect to the centre line of the adjacent shell. However in the shell descriptions in the previous section it was assumed that $\dot{\gamma}_\phi$ vanished. This assumption is invalid at such an abrupt change of geometry, and will not be made at the defect, although it will be assumed in the rest of the shell. At the defect, the plane section normal to the mid-surface plane remains planar during deformation, but is not normal to the deformed mid-surface. This approach has been used by Krenk [2], and Sih and Hagendorff [3] in strip yielding models of shells with part-through defects with pressure loading. They showed that neglecting the shear strain could give inaccurate results. They applied the higher order theory in a shallow region surrounding the defect, not just at the defect itself.

As Q_ϕ is no longer a reaction, it must be included in the yield surface. A review of yield surfaces including shear has been given by Robinson [4]. In the axisymmetric case, Q_θ is zero and N_θ and M_θ do not need to be considered at an isolated value of ϕ, as they are not necessarily continuous. Hence only N_ϕ, Q_ϕ and M_ϕ need be considered. Robinson's simplest yield surfaces, which he shows are a reasonable approximation, for shells of uniform thickness are:

limited interaction:
$$\left(\frac{N_\phi}{N_1}\right)^2 + \left(\frac{Q_\phi}{Q_1}\right)^2 \leq 1 \tag{13}$$

$$\left(\frac{M_\phi^*}{M_1}\right)^2 + \left(\frac{Q_\phi}{Q_1}\right)^2 \leq 1 \tag{14}$$

$$\text{sandwich} \quad \left(\frac{N_\phi}{N_1} \pm \frac{M_\phi^*}{M_1}\right)^2 + \left(\frac{Q_\phi}{Q_1}\right)^2 \leq 1 \tag{15}$$

$$\text{where } Q_1 = \tfrac{1}{2}\sigma_y t\eta \qquad N_1 = \sigma_y t\eta \qquad M_1 = \tfrac{1}{4}\sigma_y t^2\eta^2 \tag{16}$$

and M_ϕ^* is the moment referred to the centreline of the ligament.

$$M_\phi^* = M_\phi - \tfrac{1}{2}\zeta t(1-\eta)N_\phi \tag{17}$$

All of these yield surfaces are cylinders in stress resultant space. If a multilinear yield surface is required (as some methods, to be described later, use), these may be inscribed by polygonal cylinders. With a hexagon the maximum error around the cylinder may be minimized by choosing the vertices suitably to give a value of 15%, as in the Tresca-Mises relationship.

5. SOLUTION METHODS

Two basic methods are available:

1) Determine a statically admissible stress field, and use the lower bound theorem.
2) Determine a kinematically admissible velocity field, and use the upper bound theroem.

The criteria for admissibility at the defect will be different from the criteria in the rest of the shell. In a statically admissible stress field at the defect, Q_ϕ must be taken into account. A kinematically admissible velocity field at the defect may have discontinuities in both v_n and v_ϕ, whereas in the shell v_n must be continuous but $dv_n/d\phi$ may be discontinuous giving rise to hinge circles.

These admissible fields must then be chosen to optimize the bound. If the method used does not allow all possible admissible fields, then the two bounds will not be equal. If approximations are introduced (as by discretization), then the strict bounding nature is lost.

6. EXAMPLES

6.1 Sphere with external fully-circumferential part-through defect

The geometry for this example is shown in fig. 1. The limit pressure was calculated by three methods, using the limited interaction yield surface.

1) An analytical stress field in terms of three parameters was used, described in Goodall and Griffiths [5]. These parameters were varied to optimize the lower bound to the limit pressure.

2) The equilibrium equations were discretized using finite differences. The yield surface at the defect was linearized by inscribing a hexagonal cylinder. The limit pressure was determined by linear programming, using the stress resultants and the pressure as the independent variables. Due to the approximations introduced in discretization, the strict lower bound nature is lost.

3) The virtual work equation was discretized using the trapezoidal rule for

integration. The yield surface at the defect was linearized by circumscribing a hexagonal cylinder. The limit pressure was determined by linear programming, with the velocities as independent variables. Due to the approximations introduced in discretization, the strict upper bound nature is lost.

Experimental results are also available from Goodall and Griffiths for this geometry, giving a fourth set of values for the limit pressure.

The results of the different methods are compared in table 1, where the subscripts refer to the methods above. The test vessels failed by the lifting off of the spherical caps, which involved a large shear strain at the defect. For small values of ρ and small values of η, the limit pressure is determined by the yield criterion at the ligament. For large values of ρ, the limit pressure tends to the membrane limit pressure for a sphere with thickness equal to the ligament thickness. In comparing the experimental results with theory, the flow stress has to be arbitrarily chosen. Two choices are shown in the table. For small ρ, where the ligament dominates, the two lower bound methods agree reasonably. The upper bound method is based on circumscribing yield surface, and has a correspondingly higher limit pressure. For larger ρ, the finite difference methods agree with each other, and give a higher result than the analytic lower bound, which is more restrictive in its admissible stress fields.

In comparing with experimental results, conventionally a flow stress $\bar{\sigma}$ is used where

$$\sigma_y \leq \bar{\sigma} \leq \sigma_u$$

Two different choices of $\bar{\sigma}$ are shown in table 1. A more accurate method of including the effects of strain-hardening has been given by Ainsworth [7]. Large deformation effects are not taken into account however.

6.2 Sphere with protruding cylindrical nozzle, with external defect in sphere at intersection

The geometry for this example is shown in fig. 2.

The limited interaction yield surface, was again used, and the limit pressure was calculated, using three different methods. In each case an analytic result for the ring load on a cylinder due to Eason [6] was used. The three methods were:

1) A similar analytic stress field was used to that in the sphere, but with only one free parameter. The optimal pressure was determined analytically by the lower bound method.

2) An analytic velocity field with two free parameters was used, and the limit pressure was calculated by the upper bound method. As there are no constraints, the optimal pressure is simply determined by calculating the pressure for a range of values of the free parameters.

3) A lower bound finite difference method was used, as in the sphere geometry.

The results are compared in fig. 1. The abrupt changes in the curves are due to change in the set of active constraints and equivalently change in the deformation mechanism. As in the sphere, at small values of η the limit pressure is determined by the yield criterion in the ligament. For large values of η, the ligament thickness has no effect, and the limit pressure is determined by a mechanism in the vicinity of the sphere-cylinder intersection. The analytic lower bound solution does not show this independence of η. Both lower bound solutions show a transitional regime, where deformation occurs both in the ligament and in the shell. The velocity fields considered in the upper bound solution are not sufficiently general to demonstrate this transition. The bounds are reversed for small values of η because the defect yield criterion is approximate. The pressures are normalized with respect to the membrane limit pressure of the plain sphere. They do not approach unity at $\eta=1$ because of the weakening effect of the nozzle.

7. CONCLUSIONS

The limit load of structures containing defects is a quantity used in two-criteria structural integrity assessments. In order to assist with routine calculations, the literature has been surveyed, and extra solutions added to form a compendium of solutions. The method of calculation is illustrated here by considering the limit pressure of two axisymmetric shell geometries. Standard shell approximations are used, except that the shear strain at the defect is not neglibible, and the shear stress resultant at the defect needs to be included in the yield function. The limit pressure of cracked spheres and spheres with protruding cylindrical nozzles have been calculated by general purpose linear programming methods, and by ad hoc semi-analytical methods, using both the lower and upper bound theorems of limit analysis. These give different approximations which have been compared. What is strictly needed for an accurate representation of ductile fracture is a plastic instability analysis. Limit analysis is an approximation to this.

REFERENCES

[1] HODGE, P.G., "Limit analysis of rotationally symmetric plates and shells', Prentice-Hall, 1963.

[2] KRENK, S., "Influence of transverse shear of an axial crack in a cylindrical shell", Int.J.Fracture, 14, pp. 123-143 (1978).

[3] SIH, G.C., HAGENDORFF, H.C., "A new theory of spherical shells with cracks", pp. 519-545 of "Thin shell structures', ed. Y.C. Fung and E.E. Sechler (Symposium at Caltech 1972), Prentice-Hall, 1974.

[4] ROBINSON, M., "The effect of transverse shear stresses on the yield surface for thin shells", Int. J. Solids Structures 9, pp. 819-828 (1973).

[5] GOODALL, I.W., GRIFFITHS, J.E., "On the limit analysis of a spherical pressure vessel with fully circumferential defects", Int.J.Mech.Sci., 24, pp. 635-645 (1982).

[6] EASON, G., "The load carrying capacities of cylindrical shells subjected to a ring of force", J.Mech.Phys.Solids, 7, pp. 169-181 (1959).

[7] AINSWORTH, R.A., "The assessment of defects in structures of strain hardening materials", CEGB report TPRD/B/0175/N82 (1982).

[8] MILLER, A.G., "Review of limit loads of structures containing defects", CEGB report TPRD/B/0093/N82 (1982).

[9] DOWLING, A.R., TOWNLEY, C.H.A., "The effect of defects on structural failure: a two-criteria approach", Int.J.Pres.Ves. & Piping 3, pp. 77-107 (1975).

[10] HARRISON, R.P., LOOSEMORE, K., MILNE, I., DOWLING, A.R., "Assessment of the integrity of structures containing defects", CEGB Report R/H/R6-Rev.2 (1980).

Acknowledgment

This paper is published by permission of the Central Electricity Generating Board.

Table I Limit pressures for spheres with fully circumferential defects

ρ	η	L/R	p_1	p_2	p_3	p_{exp}^{a}	p_{exp}^{b}
0.5	0.3	0.25	0.65	0.68	0.85		
1.0	0.3	0.25	0.65	0.68	0.78		
2.0	0.3	0.25	0.50	0.57	0.58		
4.0	0.3	0.25	0.37	0.46	0.46		
3.0	0.538	0.6	0.62	0.56	0.66	0.69	0.58
3.0	0.33	0.6	0.40	0.38	0.42	0.47	0.40
2.0	0.30	0.4	0.45	0.47	0.52	0.53	0.44
2.0	0.10	0.4	0.16	0.21	0.19	0.20	0.17

a) based on $\frac{1}{2}(\sigma_u + \sigma_y)$

b) based on σ_u

For geometry, see nomenclature and fig. 1.
For definition of p_i, see section 6.1.

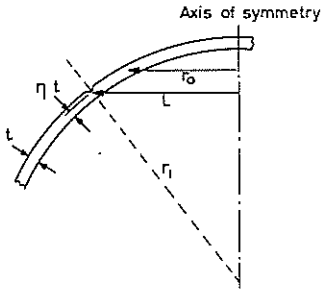

Fig. 1 Geometry for sphere.

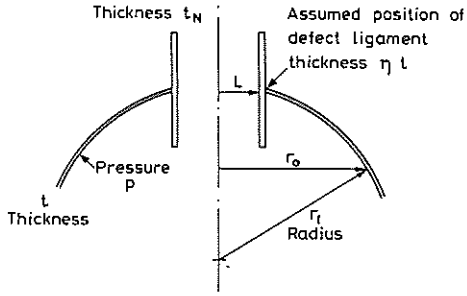

Fig. 3 Limit pressure v. ligament thickness for sphere-cylinder intersection.

$(\frac{L}{R} = 0.0861 \quad \frac{L_N}{L} = 0.857$

$\frac{R}{t} = 105 \quad \frac{t_N}{t} = 0.86)$

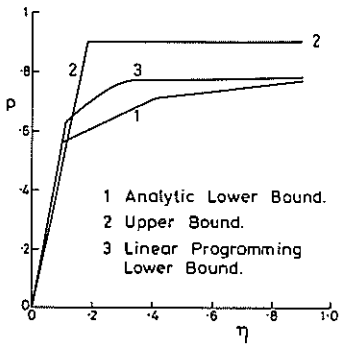

Fig. 2 Geometry for sphere-cylinder intersection.